INTRALAMINAR FRACTURE TOUGHNESS CHARACTERIZATION: A COMPUTATIONAL MICROMECHANICS PERSPECTIVE

M. Herráez[1], C. González[1,2], C.S. Lopes[1]

[1]IMDEA Materials, C/Eric Kandel 2, 28906 - Getafe, Madrid, Spain
[2]Polytechnic University of Madrid, E.T.S. de Ingenieros de Caminos, 28040 Madrid, Spain

Keywords: Computational Micromechanics, Fracture toughness, Linear Elastic Fracture Mechanics, Carbon Fibre Reinforced Polymer

Abstract

A computational micromechanics model to capture the R-curve corresponding to the intralaminar cracking process through a fibre reinforced polymer has been developed. The model combines an embedded cell approach with the Linear Elastic Fracture Mechanics (LEFM) displacement field to reproduce the crack propagation phenomenon. This strategy was previously validated through the calculation of the J-integral around the fracture process zone (FPZ). Good agreement was found between the analytical and numerical solutions in the FPZ. Two damage mechanisms were found to govern the intralaminar toughness of the composite (G_{2+}): interface debonding and matrix failure. These mechanisms were identified in the R-curves showing their own characteristic length and fracture energy.

1. Introduction

Polymer matrices reinforced with high performance fibres or FRPs are preferred candidates in structural applications where the strength to weight ratio leads the structural design process. One of the main drawbacks regarding the use of these materials is their complex mechanical behaviour, hardly predictable, which depends on the constituents properties, fibres, matrix and interfaces, as well as their spatial distribution within the material. Manufacturing conditions also play an important role and are responsible for the generation of defects in the form of voids, interfacial debonding, resin pockets or dry fibre areas which are considered detrimental for the final performance of the material [1].

Although different experimental procedures are available to obtain the ply stiffness and strength, the fracture toughness associated with each fracture mode of the ply are more difficult to determine [2]. The failure modes exhibited by laminated composites can be divided into interlaminar fracture or delamination, intralaminar fracture and translaminar fracture. Delamination has been extensively investigated over the past decades leading to standardised procedures [3]. Translaminar toughness has become a widely studied failure mode as the longitudinal direction is the one supporting higher loads either in tension [4, 5] or compression [6]. Intralaminar fracture toughness can be divided into longitudinal and transverse cracking [7], whether the crack front is normal or parallel to the fibres respectively. An alternative interesting approach to effectively analyze the effect of the constituent properties on the toughness of the composite material is the computational micromechanics (CMM). In this work, a 2D micromechanical Finite Element Model is developed to determine the intralaminar transverse fracture toughness of a uniaxially-reinforced carbon-fibre epoxy-matrix composite. The fracture toughness obtained from this

Excerpt from ISBN 978-3-00-053387-7

model will be used in a homogenized cohesive zone model (CZM) to verify its equivalent macroscopic response.

2. Numerical model

2.1. Computational Micromechanics (CMM)

The micromechanical model developed represents the fracture process zone (FPZ) ahead of the crack tip and its surroundings as an embedded-cell model [8]. The full details of the composite microstructure are resolved in the FPZ representing a random dispersion of parallel fibres embedded in a polymer matrix as the transverse section of an unidirectional composite ply [1, 9, 10]. The rest of the model is represented as a homogeneous, transversely isotropic elastic solid whose behavior is given by any suitable homogenization model.

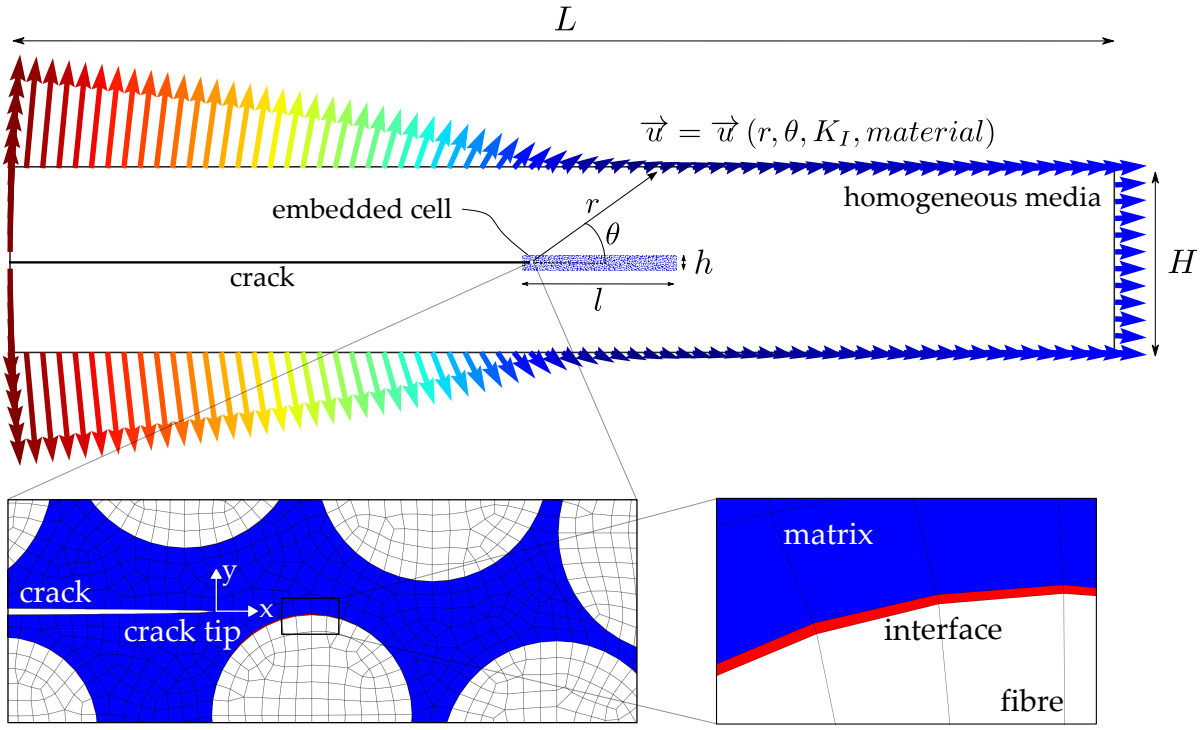

Figure 1. Schematic view of the model showing the detail of the fibres distribution, FEM mesh, cohesive interface and displacement field (LEFM)

2.1.1. Constitutive models of fibre, matrix and interfaces

The model is discretized using finite elements in Abaqus Standard [11]. The matrix, the fibres and the homogenized region are modelled with 4-node fully integrated quad isoparametric elements (CPE4). The fibre-matrix interface debonding was simulated with 4-node cohesive isoparametric elements (COH2D4) inserted at the interfaces between fibres and matrix. Perfect and homogeneous contact between fibres and matrix was assumed. Carbon fibres behave as a linear elastic and transversely isotropic solid. The thermoelastic constants of AS4 carbon fibres are reported in Table 1 [12]. Fibre matrix interface failure is taken into account using a cohesive zone model. To this end, cohesive elements inserted at the interface between fibres and matrix are governed by a mixed-mode linear traction-separation law where damage onset is controlled by the following stress criterion:

Excerpt from ISBN 978-3-00-053387-7

$$\left(\frac{\langle t_n \rangle}{N}\right)^2 + \left(\frac{t_s}{S}\right)^2 + \left(\frac{t_t}{S}\right)^2 = 1 \tag{1}$$

where $\langle\ \rangle$ stands for McCaulay brackets defined as $\langle x \rangle = \max(0, x)$, t_n is the normal traction and, t_s and t_t are the shear components of the traction vector. N is the normal strength and S is the shear strength assumed to be equal in both shear directions s and t. In addition, damage evolution is governed by a Benzeggagh-Kenane [13] law as

$$G^c = G_n^c + (G_s^c - G_n^c) \cdot \left(\frac{2G_s}{G_n + 2G_s}\right)^{\eta_{BK}} \tag{2}$$

where η_{BK} is the Benzeggagh-Kenane power exponent, G_n^c and G_s^c are the normal and shear fracture energies respectively, and G_n and G_s the reciprocal work under mixed mode propagation. The interface parameters used in the simulations are presented in Table 2 [14]. Finally, the polymer matrix behaviour is modeled using the Lubliner damaged/plasticity model included in Abaqus Standard [11]. This constitutive equation allows the material to behave as quasi-brittle when subjected to dominant tensile stress while it shows elasto-plastic behaviour under pressure confinement and compressive loads. The tensile response is, therefore, linear and elastic with elastic modulus and Poisson ratio E_m and ν_m until the tensile failure stress $\sigma_{t0} = 121$ MPa is reached. Beyond this point, a quasi-brittle softening is induced in the material being $G_t = 90\ J/m^2$ the matrix fracture energy. Under uniaxial compression the response is linear up to the initial yield limit $\sigma_{c0} = 176$ MPa. Then, stress hardening takes place until the ultimate stress value is reached $\sigma_{cu} = 180$ MPa, [8, 14]. The elastic properties of the homogenized region were derived from the fibre and matrix properties through the Chamis homogenization model [15] considering a fibre volume fraction of 65%.

Table 1. Elastic properties of the carbon fibres [12], epoxy matrix [8, 14] and the homogenized composite ($V_f = 65\%$).

Material	E_1 (GPa)	E_2 (GPa)	ν_{12}	ν_{23}	G_{12} (GPa)	G_{23} (GPa)
Fibre	231.6	12.97	0.3	0.46	11.3	4.45
Matrix	5.07	-	0.35	-	-	-
Composite	152.3	7.17	0.32	0.48	4.1	2.42

Table 2. Material properties of fibre-matrix interface [14].

N (MPa)	S (MPa)	E_{nn} (GPa)	E_{ss} (GPa)	G_n^c (J/m^2)	G_s^c (J/m^2)	η_{BK}
42	63	100	100	2	30	1.2

2.2. Linear Elastic Fracture Mechanics (LEFM)

The novelty of this model comes from the application of a prescribed displacement field along the boundary (see Fig. 1). Through this approach, the Stress Intensity Factor (SIF, K_I) is controlled in the fractured region through the application of the displacement field on the model boundaries. This displacement field corresponds to the analytical solution of the LEFM around the crack tip for a transversely isotropic elastic solid under plane strain with pure mode I load ($K_I \neq 0,\ K_{II} = 0$) according to,

Excerpt from ISBN 978-3-00-053387-7

$$\begin{Bmatrix} u_x \\ u_y \end{Bmatrix} = \frac{K_I}{2\mu} \cdot \sqrt{\frac{r}{2\pi}} \cdot (\kappa - \cos\theta) \begin{Bmatrix} \cos\frac{\theta}{2} \\ \sin\frac{\theta}{2} \end{Bmatrix} \tag{3}$$

where r and θ are the polar coordinates of the node from the crack tip (see Fig. 1), K_I is the stress intensity factor in mode I, and κ and μ are material properties defined as,

$$\kappa = \frac{3 - \nu_{23} - 4\nu_{21}\nu_{12}}{1 + \nu_{23}} = 1.70 \tag{4}$$

$$\mu = \frac{E_2}{2 \cdot (1 + \nu_{23})} = 2.42 \text{ GPa} \tag{5}$$

The intralaminar fracture energy of the composite is obtained from the stress intensity factor, K_I, through Griffith equation, $G = K_I^2/E'$, where the effective modulus, E', is written as $E' = E_2/(1 - \nu_{12}\nu_{21}) = 7.2$ GPa for transversely isotropic elastic solids.

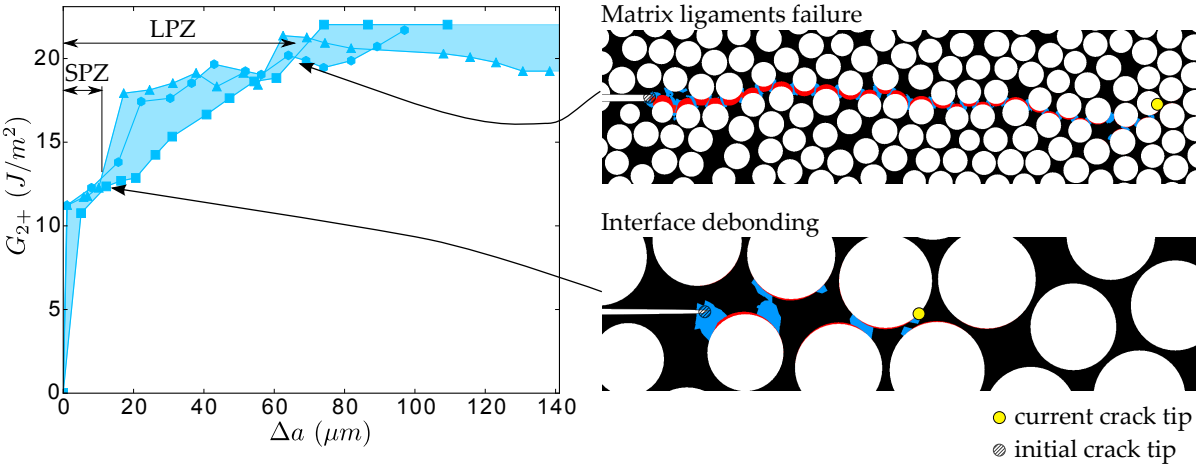

Figure 2. a) R-curve envelope obtained from three realizations. b) Illustrations of the crack propagation process identifying the two damage mechanisms: matrix plasticity (blue) and interface debonding (red).

3. Results

The intralaminar fracture propagation process was simulated using the embedded cell described in the previous section. The computed R-curve, intralaminar fracture energy (G_{2+}) vs. crack propagation (Δa), is plotted in Fig. 2. The model was able to reproduce the actual deformation and failure mechanisms at the microscopic scale. The analysis of the R-curve yields two regions with their characteristic length and fracture energy. In the first region it is observed a very short characteristic length, around $10\mu m$ (SPZ), in which the energy dissipated is 12 J/m^2, observing the failure mechanisms governing the crack propagation in that stage it can be concluded that fibre/matrix debonding is leading this initiation phase. The second region is found around a characteristic length of $70 - 80\mu m$ (LPZ), at this point the crack propagation becomes stable and is not capable of dissipating more energy ($G_{2+}^{stab} = 22$ J/m^2), this additional energy comes from the exhaustion of the bridging effect produced by the matrix ligaments. The analysis of the energy dissipated by the cohesive interface and the matrix shows that initially the fracture process is dissipated by the interfaces, but later this trend shifts to the matrix dissipation as plastic deformation (see Fig. 3b).

Excerpt from ISBN 978-3-00-053387-7

Good agreement was found between the numerical and analytical solution of the stress field (see Fig. 3a). Out of the FPZ, the agreement was excellent, while in the FPZ a similar trend was observed ($\sim r^{-1/2}$). The J-integral was computed around the FPZ to ascertain the applicability of the method in an embedded cell model with damage an plasticity material models. During the initial stages of the crack propagation the relative error was below 1%, however, as the FPZ becomes larger the relative error increases up to 5% when the FPZ is fully developed. This error is mainly dependent on the relative size of the FPZ to the full model size. This issue is related with applicability of the LEFM in problems where the autonomous region (FPZ) is much smaller than the dominion of the problem.

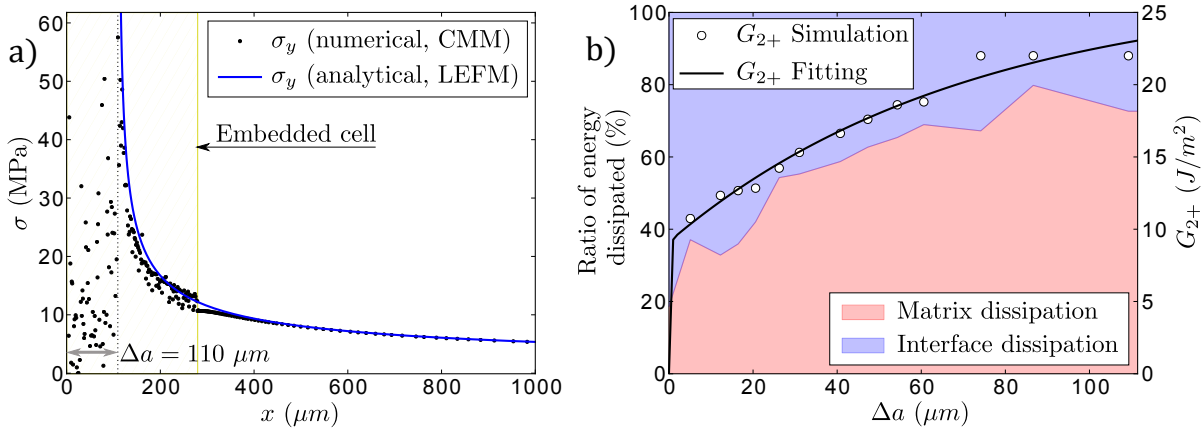

Figure 3. a) Stress profile (σ_y) along the crack plane with $\Delta a = 110\ \mu m$. b) Ratio of energy dissipated by the matrix (red) and the interfaces (blue) during crack growth and R-curve.

4. Conclusions

A novel methodology to precisely control the Stress Intensity Factor in mode I (K_I) at the crack tip through a finite elements numerical model has been developed. The numerical evaluation of the J-integral along a contour surrounding the fractured region is not required and the applied boundary conditions mimic the stress field ahead of the crack tip. In this work the intralaminar transverse fracture toughness (G_{2+}) was computed for a unidirectional composite taking advantage of the 2D problem assuming plane strain conditions. Not only the stable fracture toughness, but also the R-curve was tracked during the initiation of the crack propagation. The onset of damage is controlled by the fibre-matrix interface debonding which triggers matrix ligaments tensile failure leading to crack propagation.

Acknowledgments

The authors kindly acknowledge the support of the Spanish Ministry of Economy and Competitiveness through the project MAT201237552. C.S. Lopes acknowledges the support of the Spanish Ministry of Economy and Competitiveness through the Ramon y Cajal program.

References

[1] C. González and J. LLorca. Mechanical behavior of unidirectional fiber-reinforced polymers under transverse compression: Microscopic mechanisms and modeling. *Composites Science and Technology*, 67(13):2795–2806, October 2007.

[2] J Llorca, C González, J M Molina-Aldareguía, J Segurado, R Seltzer, F Sket, M Rodríguez, S Sádaba, R Muñoz, and L P Canal. Multiscale modeling of composite materials: a roadmap

Excerpt from ISBN 978-3-00-053387-7

towards virtual testing. *Advanced materials (Deerfield Beach, Fla.)*, 23(44):5130–47, November 2011.

[3] ASTM, D5528-13, Standard Test Method for the Mode I Interlaminar Fracture Toughness of Unidirectional Fiber-Reinforced Polymer Matrix Composites, 2013.

[4] M.J. Laffan, S.T. Pinho, P. Robinson, and L. Iannucci. Measurement of the in situ ply fracture toughness associated with mode I fibre tensile failure in FRP. Part I: Data reduction. *Composites Science and Technology*, 70(4):606–613, apr 2010.

[5] M. J. Laffan, S. T. Pinho, P. Robinson, and A. J. McMillan. Translaminar fracture toughness testing of composites: A review. *Polymer Testing*, 31(3):481–489, 2012.

[6] G. Catalanotti, J. Xavier, and P.P. Camanho. Measurement of the compressive crack resistance curve of composites using the size effect law. *Composites Part A: Applied Science and Manufacturing*, 56:300–307, jan 2014.

[7] S.T. Pinho, P. Robinson, and L. Iannucci. Developing a four point bend specimen to measure the mode I intralaminar fracture toughness of unidirectional laminated composites. *Composites Science and Technology*, 69(7-8):1303–1309, jun 2009.

[8] L.P. Canal, J. Llorca, C. González, and J. Segurado. Intraply fracture of fiber-reinforced composites: Microscopic mechanisms and modeling. *Composites Science and Technology*, 72(11):1223–1232, June 2012.

[9] E. Totry, C. González, and J. Llorca. Prediction of the failure locus of C/PEEK composites under transverse compression and longitudinal shear through computational micromechanics. *Composites Science and Technology*, 68(15-16):3128–3136, December 2008.

[10] E. Totry, J. Llorca, and C. González. Failure locus of fiber-reinforced composites under transverse compression and out-of-plane shear. *Composites Science and Technology*, 68(3-4):829–839, March 2008.

[11] Simulia, editor. *Abaqus Analysis User's Guide. Version 6.13*. 2013.

[12] M. Herráez, D. Mora, F. Naya, C.S. Lopes, C. González, and J. Llorca. Transverse cracking of cross-ply laminates: A computational micromechanics perspective. *Composites Science and Technology*, 110:196–204, February 2015.

[13] M.L. Benzeggagh and M. Kenane. Measurement of mixed-mode delamination fracture toughness of unidirectional glass/epoxy composites with mixed-mode bending apparatus. *Composites Science and Technology*, 56(4):439 – 449, 1996.

[14] F. Naya, C. González, C.S. Lopes, S. Van der Veen, and J. Llorca. Combined Multiscale Simulations in Fiber-reinforced Composites. In *ECCM16 - 16th European Conference on Composite Materials*, 2014.

[15] C.C. Chamis. Mechanics of Composite Materials: Past, Present and Future. Technical report, NASA Technical Memorandum 100793, 1984.

Excerpt from ISBN 978-3-00-053387-7